Monoterpenes as Drug Shuttles: Cytotoxic (6-Aminomethylnicotinate)dichloridoplatinum(II) Complexes with Potential To Overcome Cisplatin Resistance

Rainer Schobert,*,† Bernhard Biersack,† Andrea Dietrich,§ Antje Grotemeier,† Thomas Müller,§ Bernd Kalinowski,‡ Sebastian Knauer,† Wieland Voigt,§ and Reinhard Paschke‡

Organic Chemistry Laboratory, University of Bayreuth, Universitaetsstrasse 30, 95440 Bayreuth, Germany, Medical Faculty of the Martin-Luther-University Halle-Wittenberg, 06099 Halle, Germany, and Biocenter of the Martin-Luther-University Halle-Wittenberg, 06099 Halle, Germany

Received November 30, 2006

(6-Aminomethylnicotinate)dichloridoplatinum(II) complexes **4** esterified with terpene alcohols were tested on a panel of five human tumor cell lines. While they were accumulated in all cell lines more readily than cisplatin (CDDP), their cytotoxicities were tumor-specific and structure-dependent. Cell lines known to feature elevated levels of antiapoptotic, ion-channel-affecting proteins or otherwise impaired caspase-9 activation responded better to **4** than to CDDP, e.g., the HL-60 leukemia to the fenchyl and bornyl derivatives **4a**,**b** at an $IC_{90} \leq 10\ \mu M$. The (−)-menthyl complex **4g** was far better accumulated and more efficacious in CDDP-resistant 1411HP male germ cell tumor cells than in the congenerous CDDP-sensitive H12.1 cell line. **4g** also broke the CDDP resistance of 518A2 melanoma cells. Cell decay in each case was apoptotic as to TUNEL and Annexin V fluorescence assays. Some complexes **4** seem to positively modulate the permeability of the cell membrane and of blocked mitochondrial anion channels.

Introduction

Tumors are often intrinsically resistant to the anticancer drug cisplatin (CDDP). Acquired resistance of initially well-responding tumors and unwanted side effects are other problems that frequently thwart long-term and multidose regimens based on CDDP. Hence, various analogues of CDDP have been prepared to overcome these problems,[1−5] among them conjugates of Pt(II) complexes with cytotoxic codrugs, or bioactive shuttle components such as porphyrins,[6,7] bile acids,[8] hormones,[9] or modulators[10,11] that expedite the transmembrane transport or the drug accumulation within the cell.

Monoterpenes have received little attention as potential membrane-modulating groups. Menthol was reported to partition from the aqueous phase into various types of membranes resulting in their expansion, in increased fluidity and permeability, and in alterations of ion transport processes in microbes.[12] More specifically, it activates the Ca^{2+}-permeable channel TRPM8 (transient receptor potential melastatine family member 8) causing a sustained influx of this cation and subsequently cell death by apoptosis as was shown for the prostate cancer LNCaP.[13,14] This might even be a general effect, as the TRPM8 polypeptide was also detected in the endoplasmic reticulum and the plasma membranes of other normal and cancerous tissues and cells including melanoma, testicular, breast, and colorectal carcinoma.[15] However, recently menthol was shown to induce necrotic rather than apoptotic death of HL-60 leukemia cells *in vitro*.[16] Some other terpene alcohols were found to cause regression of various tumors in animal models or in cell culture, when administered in high doses. For instance, perillyl alcohol inhibited cell growth *in vitro* and *in vivo* of tumors including mammary, skin, and lymphoblastoma by membrane-related mechanisms and in an apoptotic way.[17−19]

Following the rationale that monoterpene platinum complex conjugates should be readily transported across cell membranes while possibly eliciting some antiproliferative effect at ion channels ahead of the DNA−platinum interaction, we prepared (6-aminomethylnicotinate)dichloridoplatinum(II) complexes linked via ester bonds to simple terpene alcohols. Their cytotoxicities against various CDDP-sensitive and -resistant tumor cell lines were assessed *in vitro* as were their uptake rates by atomic absorption spectroscopy (AAS), their effect on plasmid DNA by electrophoretic mobility measurements, and the mechanism of cell death induced by them, i.e., necrosis vs apoptosis, by fluorescence labeling assays (TUNEL[a] and Annexin V).

Results and Discussion

Chemistry. The platinum complexes **4** featuring (+)-α-fenchyl (**4a**), (−)-bornyl (**4b**), *sec*-adamantyl (**4c**), 1-methyladamantyl (**4d**), thymyl (**4e**), and cyclohexyl (**4f**) residues were prepared by a route previously described for the synthesis of the (−)-menthyl derivative **4g** (Scheme 1).[20] To evaluate the influence of the configuration of stereocenters in the terpenyl residues, three stereoisomers of **4g** were also synthesized from (+)-menthol (*ent*-**4g**), (+)-isomenthol (**4h**), and (+)-neomenthol (**4i**). Yamaguchi esterification[21] of N-Boc-protected 6-aminomethylnicotinic acid **1** with the respective alcohol afforded the esters **2**, which were deprotected with 4 M HCl in dioxane to give the ammonium chlorides **3**. These were treated with K_2PtCl_4 under slightly acidic conditions to leave the dichloridoplatinum(II) complexes **4** as yellow crystalline solids in overall yields ranging from 30 to 66% with respect to **1**.

Biological Evaluation. Table 1 compares the growth inhibitory effects of all complexes **4** on cells of the CDDP-sensitive HL-60 leukemia[22,23] and CDDP-resistant 518A2 melanoma,[24,25] two tumors known to be rich in antiapoptotic, mitochondrial

* To whom correspondence should be addressed. Phone: +49(0)921 552679. Fax: +49(0)921 552671. E-mail: Rainer.Schobert@uni-bayreuth.de.

† University of Bayreuth.

‡ Biocenter of the Martin-Luther-University Halle-Wittenberg.

§ Medical Faculty of the Martin-Luther-University Halle-Wittenberg.

[a] Abbreviations: FLUOS, 5(6)-carboxyfluorescein-*N*-hydroxysuccinimide ester; MTT, 3-(4,5-dimethylthiazol-2-yl)-2,5-diphenyltetrazolium bromide; PBS, phosphate-buffered saline; PI, propidium iodide; SRB, sulforhodamine-B; TUNEL, terminal deoxynucleotidyl transferase-mediated dUTP nick-end labeling.

10.1021/jm061379o CCC: $37.00
Published on Web 03/01/2007

Scheme 1. Synthesis of (6-Aminomethylnicotinate)dichloridoplatinum(II) Complexes **4**[a]

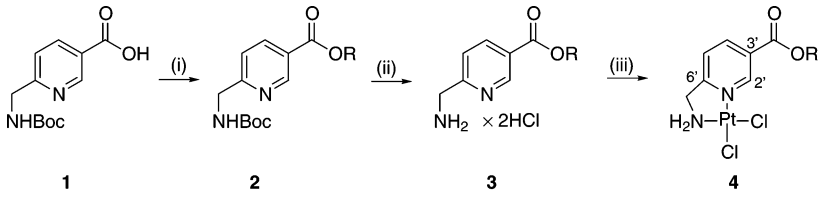

Yields / % :

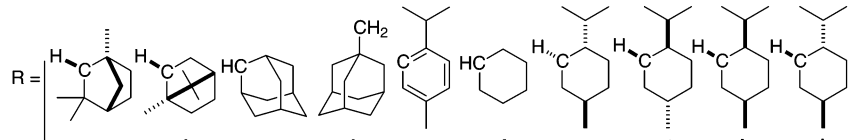

	a	b	c	d	e	f	g	*ent*-g	h	i
2	90	82	82	79	90	95		73	91	88
3	82	84	86	83	79	90		87	96	96
4	64	41	56	56	56	50		81	51	47

[a] Reagents and conditions: (i) Et_3N, $C_6H_2Cl_3COCl$, DMAP, alcohol, DMF/toluene, r.t., 16 h; (ii) 4 M HCl/dioxane, r.t., 1 h; (iii) K_2PtCl_4, H_2O/THF, r.t., 24 h.

Table 1. Inhibitory Concentrations[a] IC_{50} and IC_{90} of CDDP and Compounds **4** When Applied to HL-60 Leukemia and 518A2 Melanoma Cells

	HL-60		518A2	
compd	IC_{50}, μM	IC_{90}, μM	IC_{50}, μM	IC_{90}, μM
CDDP	3.5	>25	35	—[b]
4a	5.2 (±1.1)	9 (±3.3)	21.2 (±8.6)	—[b]
4b	5.2 (±0.9)	8.5 (±3.2)	18.1 (±0.6)	45 (±2.5)
4c	6.9 (±0.4)	10 (±4.0)	46.4 (±5.4)	—[b]
4d	20.1 (±2.9)	>40	—[b]	—[b]
4e	24.5 (±2.5)	>40	39.7 (±4.9)	—[b]
4f	—[b]	—[b]	—[b]	—[b]
4g	8 (±1.0)	15 (±3.9)	7.4 (±0.1)	15 (±0.9)
ent-**4g**	7 (±0.2)	12 (±0.7)	15.5 (±1.1)	>50
4h	14.5 (±2.7)	23 (±6.0)	30.7 (±3.9)	>50
4i	9.8 (±3.2)	25 (±5.8)	8.3 (±0.8)	>50

[a] Values are derived from dose−response curves obtained by measuring the percentage of viable cells relative to untreated controls after 24 h exposure of HL-60 leukemia and 518A2 cells to test compounds using an MTT assay. Values represent means of four independent experiments. [b] $IC_{50/90}$ not reached.

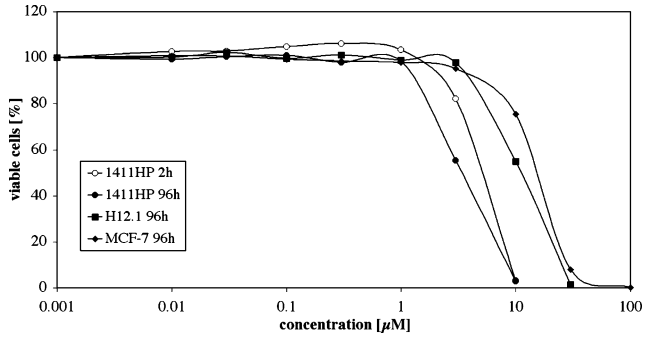

Figure 1. Concentration−response curves of treatments of cells of male germ cell tumors 1411HP and H12.1 and of MCF-7 breast cancer with **4g**. Values represent means of four independent experiments using an SRB assay; % viable cells are relative to untreated controls.

anion-channel blocking proteins such as Bcl-2. In HL-60 leukemia cells, the norbornane and adamantyl derivatives **4a**−**c** gave rise to almost congruent dose−response curves with IC_{50} values (ca. 6 μM) similar to that of CDDP but IC_{90} values (ca. 10 μM) far smaller. Like CDDP, these derivatives were significantly less active against the 518A2 melanoma cells. In contrast, the (−)-menthol derivative **4g** was equally and highly active in both cell lines. The low IC_{50} and IC_{90} doses necessary for the melanoma cells could be interpreted as a breach of their cisplatin resistance, due either to an increased uptake or a mechanism of action different from that of CDDP, such as the removal of the blockade of the mitochondrial anion channels. The complexes **4d** and **4e** were only weakly cytotoxic in HL-60 cells and not at all in the melanoma cells. The cyclohexyl derivative **4f** was virtually inactive in both cell lines. The presence of rigid bi- or tricycles or at least of conformationally fixed puckered monocycles seems to be a prerequisite for cytotoxicity. It should be mentioned that neither the free terpene alcohols nor (6-aminomethylnicotinic acid)dichloridoplatinum-(II) **4** (R = H), a potential hydrolysis product of complexes **4**, were noticeably cytotoxic (IC_{50} > 50 μM) against the tested cells. Changing the configuration of stereocenters in the terpene moieties of **4** also affected their bioactivity. The complex *ent*-**4g** exhibited activity against HL-60 identical to that of its enantiomer **4g**. However, its effect on 518A2 cells was somewhat weaker and of a greater $IC_{50/90}$ spread than that of **4g**. This phenomenon could originate from a diastereomeric discrimination in the interaction of the enantiomers with chiral, nonracemic biomolecules or structures such as membranes, proteins, or the helical DNA. The diastereomer **4h** was the one least active in both cell lines. The inhibitory effect of diastereomer **4i**, which features an axially linked (+)-neomenthyl group, came on quickly for both types of tumor cells but slackened off considerably at higher concentrations. This is represented by a flat dose−response curve and a large $IC_{50/90}$ spread.

Conjugate **4g** was then tested on cells of the male germ cell tumors H12.1 and 1411HP which had been established as an appropriate *in vitro/in vivo* model for investigating resistance to chemotherapy.[26] The intrinsic CDDP resistance of 1411HP cells is due to a drug accumulation rate inadequate to the markedly higher threshold necessary to induce apoptosis when compared to that of the CDDP-sensitive cell line H12.1. We found that the inhibitory effect of complex **4g** in 1411HP cells set on rapidly and steeply with the dose−response curves of the 2 h and the 96 h treatments not far asunder, while the CDDP-sensitive H12.1 cells responded less well (Figure 1). For reasons of comparison, Figure 1 also shows the mediocre effect of **4g** on cells of the breast cancer cell line MCF-7 which is sensitive to CDDP at rather low concentrations, but has low levels of antiapoptotic, anion-channel blocking proteins.[18]

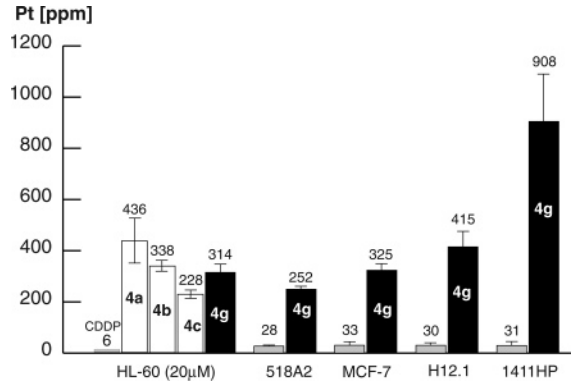

Figure 2. Drug uptake measured by atomic absorption spectroscopy (AAS) as platinum content [ppm] in lyophilized cells harvested after 2 h. Cell lines H12.1, 1411HP, MCF-7, and 518A2 were treated for 2 h with equimolar doses [30 μM] of **4g** or cisplatin (CDDP), corresponding to IC_{90} cisplatin doses for H12.1 cells. HL-60 cells were treated with 20 μM of **4a**−**c**,**g** or CDDP. Values represent means of three independent experiments.

H12.1, 1411HP, HL-60, 518A2, and MCF-7 cells were finally treated for 2 h with equimolar doses of complex **4g** or with CDDP, and the resulting platinum contents were quantified by flameless atomic absorption spectroscopy (AAS) (Figure 2). Overall, all tumor cell lines took up **4g** more readily and to a larger extent than CDDP, the resistant 1411HP cells even 2.2 times as much of it as the sensitive H12.1 cells. H12.1, 1411HP, and 518A2 cells were also treated with (+)-menthol complex *ent*-**4g** which was taken up to the same extent as **4g** within the margin of measurement accuracy. Thus, the differences in the cytotoxicities of **4g** and *ent*-**4g** on 518A2 cells are not due to an unequal accumulation. The inferior inhibitory effect of **4g** on H12.1 and MCF-7 cells when compared to CDDP cannot be ascribed to an insufficient drug uptake, either, but rather to the absence of obstacles in the mitochondrial apoptotic pathway, which **4g** would be able to alleviate.

In order to prove that compounds **4** induced indeed apoptotic rather than necrotic decay in responsive HL-60 cells we carried out TUNEL assays which allow the detection of late stages of apoptosis by labeling the 3′-OH ends of typical DNA fragments with fluorescein-tagged nucleotides.[27] These assays were conducted with cells that had been exposed to 10 μM concentrations of the respective complex **4** or CDDP for 15 h and then tested with the In Situ Cell Death Detection Kit, Fluorescein (Roche). Fluorescence microscopy revealed on average >20% TUNEL-positive, i.e., apoptotic cells upon treatment with (−)-menthol derivative **4g** while CDDP led to only <15% and negative controls to ca. 4% apoptotic cells. This is in stark contrast to the predominantly necrosis-inducing effect of free (−)-menthol on HL-60 cells.[16] Figure 3 shows typical microscopic images of HL-60 cells treated with **4g** in a TUNEL assay.

Apoptosis in HL-60 cells treated with compounds **4** was also detected by annexin V-binding assays.[28,29] Annexin V, a placental protein, binds strongly to phosphatidylserine (PS) residues in the presence of Ca^{2+}. While in living cells PS is confined to the inner membrane leaflet facing the cytosol, unavailable for binding to annexin V, in early apoptotic cells PS residues are enzymatically flipped to point toward the outside of an otherwise intact membrane, amenable to getting tagged with a fluorescein label attached to annexin V. Necrotic cells are also tagged by the annexin-V-FLUOS/PI staining kit due to their holey membranes that allow access to the inner PS residues. These necrotic as well as late apoptotic cells can be discriminated by a control staining with propidium iodide (PI) that intercalates into their DNA, while early apoptotic cells give negatives here. Due to the limited number of cells countable with the microscope, this provides only a qualitative impression of the early apoptosis vs late apoptosis/necrosis ratio. Its general trend is as follows: CDDP and the (+)-fenchyl derivative **4a** cause cell death exclusively by apoptosis. Figure 4 depicts microscopic images of HL-60 cells in annexin V/PI staining assays with the stereoisomers **4i**, **4g**, and *ent*-**4g** which are of equal cytotoxic efficacy. The images are an overlay of the red and green channels with green dots representing early apoptotic cells and the yellow (i.e., red from PI plus green from annexin staining) dots indicating necrotic or late apoptotic cells. In short, at least 2/3 of the dying cells in assays with **4a**−**c** and **4g**−**i** suffered early apoptosis. Since our TUNEL assays had shown that cells incubated with **4g** can reach late apoptotic stages as a rule, we suggest that yellow dots in the annexin-V tests are also likely to represent late apoptotic rather than necrotic cells.

Finally we tested whether the overall cytotoxicity of compounds **4** is determined by their ability to cause irreparable DNA lesions. They were incubated at different concentrations with pBR322 plasmid DNA, and the effect on the electrophoretic mobilities of the various DNA forms present was monitored (Figure 5). Generally, the bands tend to get darker toward higher complex concentrations, as the staining agent ethidium bromide can intercalate less effectively into the platinum-laden, unwound DNA. In accordance with their pronounced inhibitory effects on HL-60 cells, CDDP and the complexes **4a** and **4b** gave rise to a strong retardation of the frontmost, covalently closed circular (ccc) form due to an unwinding of the supercoiled DNA. The less active complexes **4d**−**f** did not alter the electrophoretic DNA mobilities. Only minute differences were found in the effects of the enantiomeric complexes **4g** and *ent*-**4g** on the superhelical plasmid DNA, which were weaker than those of **4a** and **4b**. Subtler gradations in the cytotoxicity patterns of **4** were not mirrored by these experiments. No correlation at all can be made with the effects on the melanoma cells. Though a prerequisite for the inhibitory activity of CDDP, the DNA−complex interaction is apparently not determining for the cytotoxicity of the complexes **4g** and *ent*-**4g** *in vitro*.

Conclusions

The terpenyl moieties in (6-aminomethylnicotinate)dichloridoplatinum(II) complexes **4a**−**c** and **4g** obviously fulfill a transmembrane shuttle function and increase significantly the rate and extent of the uptake of these conjugates into various cisplatin-sensitive and -resistant tumor cell lines when compared to CDDP. The growth inhibitory effect of these complexes, and of **4g** in particular, is most impressive in cell lines with elevated thresholds in the activation of their mitochondrial apoptotic machinery, such as 1411HP germ cell tumor or 518A2 melanoma. This is possibly due to an accessory modulation of the mitochondrial membrane or its anion channels by these complexes. The fact that they induce predominantly apoptotic cell death corroborates this assumption. The intrinsic cytotoxicity of **4g** appears to be lower than that of CDDP, as it is less efficacious in cell lines of MCF-7 breast cancer and H12.1 germ cell tumor, despite its enhanced uptake. These two cell lines are CDDP-sensitive and feature low levels of antiapoptotic ion-channel-affecting proteins. Although all active conjugate complexes **4** were found to be also good plasmid DNA binders, the differences in their cytotoxicities against various cell lines are not congruently mirrored by the electrophoretic shift assays which in fact again underscores the involvement of membrane-related phenomena. The breach of the CDDP resistance in the

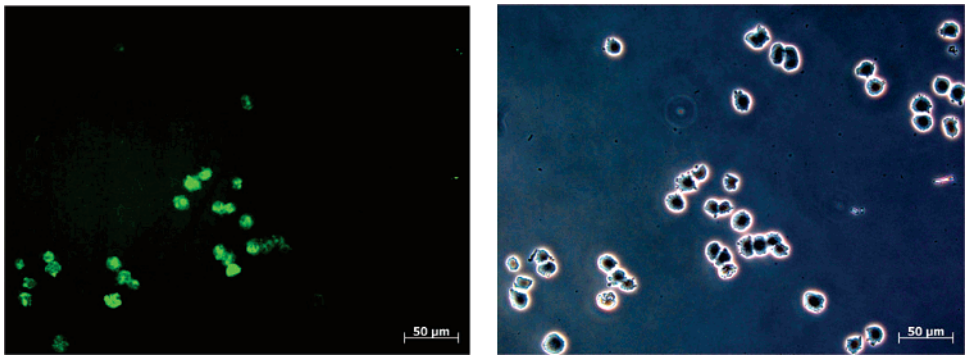

Figure 3. HL-60 cells exposed to 10 μM **4g** for 15 h and then tested with the TUNEL assay. Left: fluorescence image (excitation: 450−500 nm; detection: 515−565 nm), green fluorescent spots indicate apoptotic cells; right: same sample in the visible channel revealing all cells.

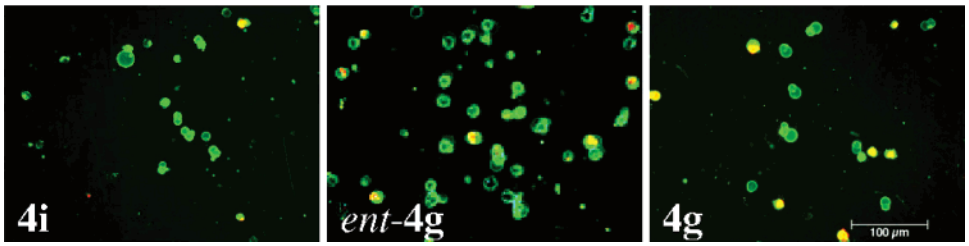

Figure 4. HL-60 cells exposed to 50 μM of **4i**, *ent*-**4g**, and **4g** for 10 h and then incubated with 30 μL of Annexin V/PI solution, consisting of 0.0192% Annexin V solution, 0.0192% propidium iodide solution, and 99.9615% incubation buffer for 10−12 min. Bright green fluorescent dots indicate early apoptotic, and yellow dots late apoptotic or necrotic cells.

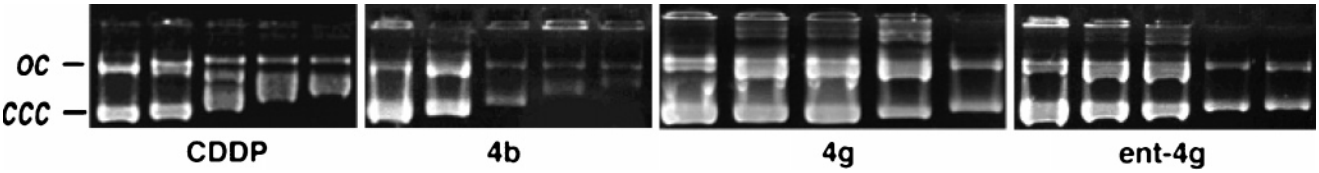

Figure 5. Modification of gel electrophoretic mobility of pBR322 plasmid DNA when incubated with differently concentrated solutions of selected complexes **4** and CDDP in DMSO (oc = open circular, ccc = covalently closed circular DNA form). Concentrations (in μM): lane 1(leftmost): 0, lane 2: 5, lane 3: 20, lane 4: 40, lane 5: 60.

518A2 melanoma cells by complex **4g** and the good response of the CDDP-resistant 1411HP germ cell tumor cells to it are remarkable. Further investigations are underway to better understand the mechanism of action and to optimize the efficacy of terpenyl conjugates of type **4**.

Experimental Section

Chemistry. α-Fenchyl 6′-(*tert*-Butoxycarbonylaminomethyl)-nicotinate (2a). Typical Procedure. Compound **1**[20] (160 mg, 0.63 mmol) was dissolved in DMF (2 mL) and treated with Et_3N (100 μL, 0.72 mmol) and 2,4,6-trichlorobenzoyl chloride (111 μL, 0.72 mmol). The resulting suspension was stirred under argon at room temperature for 20 min. A solution of (+)-α-fenchol (118 mg, 0.76 mmol) and DMAP (155 mg, 1.26 mmol) in toluene (20 mL) was added, and the resulting mixture was stirred under argon at room temperature for 16 h. After dilution with ethyl acetate and washing with water, the organic phase was dried (Na_2SO_4) and concentrated in vacuum. The residue was purified by column chromatography on silica gel 60 to leave **2a** as a colorless oil (220 mg, 0.57 mmol, 90%); R_f 0.25 (hexane/ethyl acetate 3:1); ν_{max} (ATR)/cm^{-1} 2958, 1716, 1598, 1366, 1282, 1167, 1117, 1030, 757; ^{1}H NMR (300 MHz, $CDCl_3$) δ 0.78 (s, 3H), 1.06 (s, 3H), 1.13 (s, 3H), 1.2−1.9 (m, 16H), 4.46 (d, J = 5.6 Hz, 2H), 4.58 (s, 1H), 5.6−5.7 (m, 1H), 7.33 (d, J = 8.1 Hz, 1H), 8.22 (d, J = 8.1 Hz, 1H), 9.13 (s, 1H); ^{13}C NMR (75 MHz, $CDCl_3$) δ 19.4, 20.2, 25.8, 26.8, 28.3, 29.7, 39.8, 41.4, 45.8, 48.3, 48.6, 79.6, 87.2, 121.1, 125.1, 137.6, 150.3, 155.9, 161.9, 165.4; *m*/*z* (%) (EI) 388 (5) [M$^+$], 333 (100), 197 (40), 179 (82), 135 (52).

Fenchyl 6′-Aminomethylnicotinate Bis(hydrochloric acid) (3a). Typical Procedure. Compound **2a** (210 mg, 0.54 mmol) was treated with 4 M HCl/dioxane (10 mL) at room temperature for 1 h. The formed colorless precipitate was collected, washed with diethyl ether, and dried. Yield: 160 mg (0.44 mmol, 82%); colorless solid of mp 156 °C; ν_{max} (ATR)/cm^{-1} 2951, 2872, 1717, 1463, 1295, 1133, 987, 757; ^{1}H NMR (300 MHz, DMSO-d_6) δ 0.79 (s, 3H), 1.08 (s, 3H), 1.14 (s, 3H), 1.2−2.0 (m, 7H), 4.2−4.4 (m, 2H), 4.57 (s, 1H), 7.70 (d, J = 8.2 Hz, 1H), 8.40 (d, J = 8.2 Hz, 1H), 8.5−8.7 (m, 3H), 9.11 (s, 1H); ^{13}C NMR (75 MHz, DMSO-d_6) δ 19.2, 20.1, 25.5, 26.4, 29.5, 40.8, 42.7, 47.7, 48.1, 86.6, 122.8, 125.2, 137.7, 149.3, 158.0, 164.7; *m*/*z* (%) (EI) 288 (28), 135 (100), 81 (20).

***cis*-Dichlorido[(+)-fenchyl 6′-aminomethylnicotinate]platinum(II) (4a). Typical Procedure.** A solution of **3a** (150 mg, 0.42 mmol) in H_2O (10 mL) was treated with K_2PtCl_4 (174 mg, 0.42 mmol), dissolved in H_2O. The resulting colorless precipitate was redissolved by adding THF. The pH value was adjusted to 5−6 with aqueous NaOH, and the mixture was stirred at room temperature for 24 h. The formed yellow precipitate was collected, washed with water and diethyl ether, and dried. Yield: 152 mg (0.27 mmol, 64%); mp >250 °C; $[\alpha]_D^{25}$ 11.4 (*c* 1.0, DMF); Anal. ($C_{17}H_{24}Cl_2N_2O_2Pt$) C, H, N. ν_{max} (ATR)/cm^{-1} 3229, 2954, 1728, 1288, 1127; ^{1}H NMR (300 MHz, DMF-d_7) δ 0.85 (s, 3H), 1.12 (s, 3H), 1.17 (m, 3H), 1.2−2.0 (m, 7H), 4.49 (d, J = 5.9 Hz, 2H), 4.63 (s, 1H), 6.3−6.4 (m, 2H), 7.93 (d, J = 8.2 Hz, 1H), 8.72 (d, J = 8.2 Hz, 1H), 9.98 (s, 1H); ^{13}C NMR (75 MHz, DMF-d_7) δ 19.1, 20.2, 25.9, 26.8, 40.0, 41.3, 48.5, 48.8, 53.7, 87.9, 122.7, 127.1, 138.9, 148.5, 163.9, 170.9; ^{195}Pt NMR (64.4 MHz, DMF-d_7) δ 2440; *m*/*z* (%) (EI) 288 (22), 135 (100), 81 (78).

Biological Studies. 1. Cytotoxicity Assays. Cell Lines and Culture Conditions. The human MCF-7 (HTB 22) breast cancer

cells were obtained from the American Type Culture Collection (ATCC), Rockville, MD, and the human HL-60 leukemia cells from the German National Resource Center for Biological Material (DSMZ), Braunschweig, while the human 518A2[30] melanoma cells as well as the testicular germ cell tumor cell lines H12.1[31] and 1411HP[32] were cultured in the department of oncology and hematology, Medical Faculty of the Martin-Luther University, Halle, Germany.

SRB Assay. Dose−response curves of the cell lines exposed to drug concentrations of 0.01−100 μM were established using the sulforhodamine-B (SRB) microculture colorimetric assay[33] and performed as previously described.[26] Briefly, cells were seeded into 96-well plates on day 0, at cell densities previously determined to ensure exponential cell growth during the period of the experiment. On day 1, cells were treated with the drugs dissolved in DMF to give the appropriate concentrations for indicated times, and the percentage of surviving cells relative to untreated controls was determined on day 5.

MTT Assay. MTT [3(4,5-dimethylthiazol-2-yl)2,5-diphenyltetrazolium bromide] was used to identify viable cells which are capable of reducing it in their mitochondria by succinate dehydrogenase to a violet formazan product. HL-60 leukemia cells (0.5×10^6 cells/mL) were seeded and cultured for 24 h on 96-well microplates, and the adherent 518A2 melanoma cells (5×10^4 cells/cm^2) were cultured for 24−48 h depending on growth progress. Incubation (5% CO_2, 95% humidity, 37 °C) of cells following treatment with the test compounds was continued for 24 h. Blank and solvent controls were incubated under identical conditions. Then a 5 mg/mL stock solution of MTT in phosphate-buffered saline (PBS) was added to a final MTT concentration of 0.5 mg/mL. After 2 h the precipitate of formazan crystals was redissolved in a 10% solution of sodium dodecylsulfate (SDS) in DMSO containing 0.6% acetic acid in the case of the HL-60 cells. For the adherent melanoma cells, the microplates were swiftly turned to discard the medium prior to adding the solvent mixture. The microplates were gently shaken in the dark for 30 min and left in the incubator overnight, to ensure a complete dissolution of the formazan, and finally the absorbance at wavelength 570−630 nm was measured using an ELISA plate reader (BIO-TEK, Power Wave × 340). All experiments were carried out in quadruplicate, and the percentage of viable cells quoted was calculated as the mean ± SD with respect to the controls set to 100%.

2. Fluorescence Labeling Assays. TUNEL Assay. The TdT-mediated dUTP nick-end labeling (TUNEL; Roche) assay identifies apoptosis by tagging the 3′-OH ends of DNA fragments with fluorescein.[27] A modification described by Jobmann was used.[29] HL-60 cells were incubated for 15 h with the test compounds, and aliquots of 3×10^6 cells were withdrawn and washed/centrifuged three times in 200 μL PBS. The cells were fixed by suspending in 200 μL of a freshly prepared solution of 2% formalin in PBS and shaking for 10 min at room temperature. After washing with another two 200 μL portions of PBS, 10 μL of the cell suspension was applied onto a microscope slide and air-dried at room temperature. The cells were washed by covering with PBS for 5 min, treated with a solution of 0.1% Triton X-100 in 0.1% sodium citrate, and incubated on ice for 2 min. After washing two times with PBS, 10 μL of the freshly prepared TUNEL reaction mixture, consisting of 1 μL of TUNEL-Enzyme solution and 9 μL of TUNEL-Label solution, was dropped on the cells which were then covered and incubated (5% CO_2, 95% humidity) in the dark at 37 °C for 30 min. The cells were washed three times with PBS and then analyzed by fluorescence microscopy at an excitation wavelength of 450−500 nm. The percentage of apoptotic, TUNEL-positive, green-stained cells was counted and calculated for 300 cells and expressed as mean ± SD of three independent experiments.

Qualitative Annexin V-binding assay using the Annexin-V-FLUOS Staining Kit, Roche: A 250 μL amount of a 0.5×10^6/mL cell suspension was incubated with 27.8 μL of a 500 μM stock solution (10% DMF/90% PBS) of the test compound, resulting in a final test compound concentration of 50 μM. After incubation for 10 h (37 °C, 5% CO_2, 95% humidity), the cells were centrifuged and washed with PBS twice. A 30 μL amount of Annexin V/PI solution, consisting of 0.0192% Annexin-V-Fluorescein solution, 0.0192% propidium iodide solution, and 99.9615% incubation buffer was added, and cells were incubated at room temperature in the dark for 10−12 min. For analysis by fluorescence microscopy, 25 μL of cell suspension was spread on a microscope slide.

3. Platinum Uptake by Flameless Atomic Absorption Spectroscopy. Cellular platinum concentrations were determined by flameless atomic absorption spectroscopy using a solid sampling graphite furnace atomic absorption spectrometer (SS-GF AAS) model AAS5 EA solid (Jena GmbH, Germany). A 10 mL amount of a HL-60 cell suspension (0.5×10^6/mL) was incubated with the test compounds at a concentration of 20 μM (0.4% DMF) for 2 h. Cells were centrifuged at 1200 rpm, 4 °C, 5 min, washed with PBS twice, and then freeze-dried and stored at −80 °C. The adherently growing H12.1, 1411HP, MCF-7, and 518A2 cells were treated with 30 μM of compounds for 2 h, washed, harvested by trypsinization, and freeze-dried. Prior to measurement, the cells were lyophilized and then submitted to a temperature ramp ranging from 100 to 2550 °C, atomized, and analyzed at $\lambda = 265.9$ nm.

4. Interaction of compounds 4 with pBR322 plasmid DNA was studied by agarose gel electrophoresis following the general method by Huq.[34] Briefly, 20 μL aliquots of a stock TE buffer solution of pBR322 plasmid DNA (Carl Roth GmbH, Karlsruhe, Germany; concn: 73.5 μg/mL) were incubated in the presence of increasing concentrations of CDDP and complex compounds **4** (0, 5, 20, 40, 60 μM). Incubation was carried out in the dark at 37 °C for 24 h. Each assay was treated with 2 μL of loading buffer, 11 μL of the resulting mixture containing 0.735 μg of plasmid DNA was loaded onto a 1% agarose gel, and electrophoresis was carried out in a half-concentrated trisborate-EDTA (TBE) buffer for 4 h at 66 V. At the end of electrophoresis, the gel was stained in the same buffer containing ethidium bromide (0.5 μg/mL) and visualized under UV light (using gel documentation, LTF Labortechnik and UV-Transilluminator, Vilber Lourmat).

Acknowledgment. This work was supported by a grant from the Deutsche Forschungsgemeinschaft (Scho 402/8).

Supporting Information Available: Purity data for all new compounds, syntheses and characterization of derivatives **b**−**f**, *ent*-**g**,**h**,**i** of compounds **2**−**4**. This material is available free of charge via the Internet at http://pubs.acs.org.

References

(1) Voigt, W.; Dietrich, A.; Schmoll, H.-J. Cisplatin und seine Analoga. *Pharm. Unserer Zeit* **2006**, *35*, 134−143.
(2) Reedijk, J. Bioinorganic chemistry special feature: new clues for platinum antitumor chemistry: kinetically controlled metal binding to DNA. *Proc. Natl. Acad. Sci. U.S.A.* **2003**, *100*, 3611−3616.
(3) Lippert, B., Ed. *Cisplatin: Chemistry and Biochemistry of a Leading Anticancer Drug*; Wiley-VCH: Weinheim, 1999.
(4) Wong, E.; Giandomenico, C. M. Current status of platinum-based antitumor drugs. *Chem. Rev.* **1999**, *99*, 2451−2466.
(5) Xin Zhang, C.; Lippard, S. J. New metal complexes as potential therapeutics. *Curr. Opin. Chem. Biol.* **2003**, *7*, 481−489.
(6) Brunner, H.; Schellerer, K.-M. New porphyrin platinum conjugates for the cytostatic and photodynamic tumor therapy. *Inorg. Chim. Acta* **2003**, *350*, 39−48.
(7) Lottner, C.; Bart, K.-C.; Bernhardt, G.; Brunner, H. Hematoporphyrin-derived soluble porphyrin-platinum conjugates with combined cytotoxic and phototoxic antitumor activity. *J. Med. Chem.* **2002**, *45*, 2064−2078.
(8) Paschke, R.; Kalbitz, J.; Paetz, C.; Luckner, M.; Mueller, T.; Schmoll, H.-J.; Mueller, H.; Sorkau, E.; Sinn, E. Cholic acid−carboplatin compounds (CarboChAPt) as models for specific drug delivery: synthesis of novel carboplatin analogous derivatives and comparison of the cytotoxic properties with corresponding cisplatin compounds. *J. Inorg. Biochem.* **2003**, *94*, 335−342.
(9) Descôteaux, C.; Provencher-Mandeville, J.; Mathieu, I.; Perron, V.; Mandal, S. K.; Asselin, E.; Bérubé, G. Synthesis of 17β-estradiol platinum(II) complexes: biological evaluation on breast cancer cell lines. *Bioorg. Med. Chem. Lett.* **2003**, *13*, 3927−3931.

(10) Bowler, B. E.; Ahmed, K. J.; Sundquist, W. I.; Hollis, L. S.; Whang, E. E.; Lippard, S. J. Synthesis, characterization, and DNA-binding properties of (1,2-diaminoethane)platinum(II) complexes linked to the DNA intercalator acridine orange by trimethylene and hexamethylene chains. *J. Am. Chem. Soc.* **1989**, *111*, 1299−1306.
(11) Gibson, D.; Mansur, N.; Gean, K. F. Preparation, characterization, and antitumor properties of cis-$PtCl_2$ complexes linked to anthraquinones through position number 2. *J. Inorg. Biochem.* **1995**, *58*, 79−88.
(12) Trombetta, D.; Castelli, F.; Sarpietro, M. G.; Venuti, V.; Cristani, M.; Daniele, C.; Saija, A.; Mazzanti, G.; Bissignano, G. Mechanisms of antibacterial action of three monoterpenes. *Antimicrob. Agents Chemother.* **2005**, *49*, 2474−2478.
(13) Zhang, L.; Barritt, G. J. Evidence that TRPM8 is an androgen-dependent Ca^{2+} channel required for the survival of prostate cancer cells. *Cancer Res.* **2004**, *64*, 8365−8373.
(14) Thebault, S.; Lemonnier, L.; Bidaux, G.; Flourakis, M.; Bavenkoffe, A.; Gordienko, D.; Roudbaraki, M.; Delcourt, P.; Panchin, Y.; Shuba, Y.; Skryma, R.; Prevarskaya, N. Novel role of cold/menthol-sensitive transient receptor potential melastatine family member 8 (TRPM8) in the activation of store-operated channels in LNCaP human prostate cancer epithelial cells. *J. Biol. Chem.* **2005**, *280*, 39423−39435.
(15) Zhang, L.; Barrit, G. J. TRPM8 in prostate cancer cells: a potential diagnostic and prognostic marker with a secretory function? *Endocrine-related Cancer* **2006**, *13*, 27−38.
(16) Lu, H.-F.; Hsueh, S.-C.; Yu, F.-S.; Yang, J.-S.; Tang, N.-Y.; Chen, S.-C.; Chung, J.-G. The role of Ca^{2+} in (−)-menthol-induced human promyelocytic leukemia HL-60 cell death. *In Vivo* **2006**, *20*, 69−76.
(17) Yuri, T.; Danbara, N.; Tsujita-Kyutoku, M.; Kiyozuka, Y.; Senzaki, H.; Shikata, N.; Kanzaki, H.; Tsubura, A. Perillyl alcohol inhibits human breast cancer cell growth in vitro and in vivo. *Breast Cancer Res. Treat.* **2004**, *84*, 251−260.
(18) Ariazi, E. A.; Satomi, Y.; Ellis, M. J.; Haag, J. D.; Shi, W.; Sattler, C. A.; Gould, M. N. Activation of the transforming growth factor β signaling pathway and induction of cytostasis and apoptosis in mammary carcinomas treated with the anticancer agent perillyl alcohol. *Cancer Res.* **1999**, *59*, 1917−1928.
(19) Belanger, J. T. Perillyl alcohol: applications in oncology. *Altern. Med. Rev.* **1998**, *3*, 448−457.
(20) Schobert, R.; Biersack, B. cis-Dichloroplatinum(II) complexes with aminomethylnicotinate and -isonicotinate ligands. *Inorg. Chim. Acta* **2005**, *358*, 3369−3376.
(21) Inanaga, J.; Hirata, K.; Saeki, H.; Katsuki, T.; Yamaguchi, M. A rapid esterification by means of mixed anhydride and its application to large-ring lactonization. *Bull. Chem. Soc. Jpn.* **1979**, *52*, 1989−1993.
(22) Tsujimoto, Y.; Shimizu, S. VDAC regulation by the Bcl-2 family of proteins. *Cell Death Differ.* **2000**, *7*, 1174−1181.
(23) Shimizu, S.; Narita, M.; Tsujimoto, Y. Bcl-2 family proteins regulate the release of apoptogenic cytochrome c by the mitochondrial channel VDAC. *Nature* **1999**, *399*, 483−487.
(24) Selzer, E.; Schlagbauer-Wadl, H.; Okamoto, I.; Pehamberger, H.; Potter, R.; Jansen, B. Expression of Bcl-2 family members in human melanocytes, in melanoma metastases and in melanoma cell lines. *Melanoma Res.* **1998**, *8* (3), 197−203.
(25) Jansen, B.; Wacheck, V.; Heere-Ress, E.; Schlagbauer-Wadl, H.; Hoeller, C.; Lucas, T.; Hoermann, M.; Hollenstein, U.; Wolff, K.; Pehamberger, H. Chemosensitisation of malignant melanoma by Bcl-2 antisense therapy. *The Lancet* **2000**, *356*, 1728−1733.
(26) Müller, T.; Voigt, W.; Simon, H.; Frühauf, A.; Bulankin, A.; Grothey, A.; Schmoll, H.-J. Failure of activation of caspase-9 induces a higher threshold for apoptosis and cisplatin resistance in testicular cancer. *Cancer Res.* **2003**, *63*, 513−521.
(27) Gavrieli, Y.; Sherman, Y.; Ben-Sasson, S. A. Identification of programmed cell death in situ via specific labeling of nuclear DNA fragmentation. *J. Cell Biol.* **1992**, *119* (3), 493−501.
(28) Van Engeland, M.; Nieland, L. J. W.; Ramaekers, F. C. S.; Schutte, B.; Reutelingsperger, C. P. M. Annexin V-affinity assay: a review on an apoptosis detection system based on phosphatidylserine exposure. *Cytometry* **1998**, *31*, 1−9.
(29) Jobmann, M. Apoptose bei strukturellen Herzmuskelerkrankungen. Ph.D. Thesis, University of Marburg, Germany, 2002, pp 31−32.
(30) Versteeg, R.; Noordmeer, I. A.; Krüse-Wolters, M.; Ruiter, D. J.; Schrier, P. I. C-myc down-regulates class I HLA expression in human melanomas. *EMBO J.* **1988**, *7* (4), 1023−1029.
(31) Casper, J.; Schmoll, H.-J.; Schnaidt, U.; Fonatsch, C. Cell lines of human germinal cancer. *Int. J. Androl.* **1987**, *10*, 105−113.
(32) Vogelzang, N. J.; Bronson, D.; Savino, D.; Vessella, R. L.; Fraley, E. F. A human embryonal-yolk sac carcinoma model system in athymic mice. *Cancer* **1985**, *55*, 2584−2593.
(33) Papazisis, K. T.; Geromichalos, G. D.; Dimitriadis, K. A.; Kortsaris, A. H. Optimization of the sulforhodamine B colorimetric assay. *J. Immunol. Methods* **1997**, *208*, 151−158.
(34) Chowdhury, M. A.; Huq, F.; Abdullah, A.; Bearle, P.; Fisher, K. Synthesis, characterization and binding with DNA of four planaramineplatinum(II) complexes of the forms: *trans*-PtL_2Cl_2 and $[PtL_3Cl]Cl$, where L = 3-hydroxypyridine, 4-hydroxypyridine and imidazo(1,2-α)pyridine. *J. Inorg. Biochem.* **2005**, *99*, 1098−1112.

JM061379O